CHAPTER 10
MOSFET-BASED BIOELECTRONIC DEVICES: BIOSENSORS

The MOSFET (see Chap. 9) is the basis for the development of a series of sensors for the measurement of physical and chemical parameters. The equations of the MOSFET drain current exhibit a number of parameters that can be directly influenced by external quantities, and small technological variations of the original MOSFET configuration also give rise to a large number of sensing properties. All the devices exhibit the common property that a surface charge is measured on a silicon chip, depending on an electric field in the adjacent insulator.

MOSFET-based sensors such as the GASFET, OGFET, ADFET, SAFET, CFT, PRESSFET, ISFET, CHEMFET, REFET, ENFET, IMFET, BIOFET, and others are widely discussed in Refs. 1 to 3.

In this chapter we are not trying to review the literature in the area of biosensors, since that would constitute a book in itself. The purpose is to provide an introduction to this field, with emphasis on MOSFET-based sensors. The reader should bear in mind that the field of biosensors includes many kinds of devices which are not based on MOSFET technology, such as those based on screen printing technology or fiber-optic technology. A short overview of different kinds of biosensors is given in the first section of the chapter. The interested reader can find comprehensive descriptions of the topic in Refs. 2 to 5.

Then, we will describe, as an example, the operational mechanisms of three MOS technology-based potentiometric biosensors: the ISFET (ion-sensitive field-effect transistor), the ENFET (enzyme field-effect transistor), and the LAPS (light-addressable potentiometric sensor).

10.1 BIOSENSOR OVERVIEW

The *biosensor* was first described by Clark and Lyons in 1962,[6] when the term *enzyme electrode* was used. In this first enzyme electrode, an oxido-reductase enzyme was held next to a platinum electrode in a membrane sandwich as shown in Fig. 10.1. The platinum anode polarized at +0.6 V responded to the peroxide produced by the enzyme reaction with the substrate. The primary target substrate for this system was glucose, and it led to the development of the first glucose analyzer for the measurement of glucose in whole blood. The same technique has since then been used for many other oxygen-mediated oxido-reductase enzyme systems.

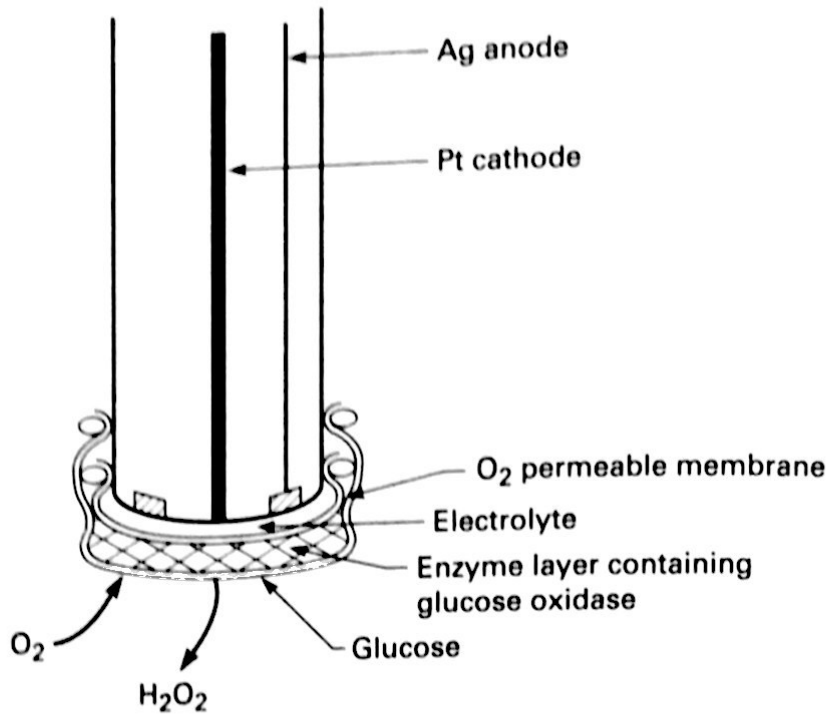

FIGURE 10.1 Modification of the Clark oxygen electrode to give an enzyme electrode.

Biosensors are small analytical bioelectronic devices that combine a *transducer* with a *sensing biological component* (biologically active substance). The transducer, which is in intimate contact with the biologically sensitive material, can be one for measuring weight, electrical charge, potential, current, temperature, or optical activity. The biologically active species can be an enzyme, a multienzyme system, an antibody or an antigen, a receptor, a population of bacterial or even eucaryotic cells, or whole slices of mammalian or plant tissue, to name a few. Substances such as sugars, amino acids, alcohols, lipids, nucleotides, and others can be specifically identified and their concentration measured by these devices.

A schematic functional representation of a biosensor is shown in Fig. 10.2. It consists

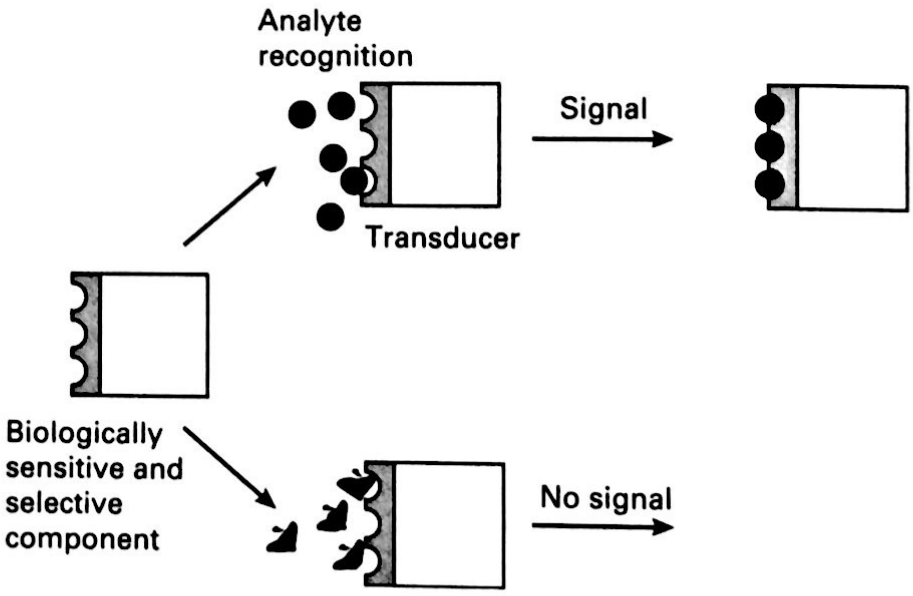

FIGURE 10.2 Schematic functional representation of a biosensor.

of a biological sensing element in close proximity or integrated with a signal transducer, to produce a reagentless sensing system specific for the target analyte.

Each component of the biosensor, its characteristics and applications will be investigated in this section.

10.1.1 Biological Component

The *biological component* of the biosensor, which represents the molecular detecting element, is made of highly specialized macromolecules (antibodies, antigens, enzymes, receptors) or of complex systems (cells, tissues) with the appropriate specificity and sensitivity. Biosensors can be classified according to the biocomponent used for detection and sensing. Examples are given for the following biological components:

Enzymes. Enzymes (see Sec. 5.4.2) are proteins that lower the energy threshold at which a given reaction takes place (catalytic function). The molecule being modified (e.g., oxidized, reduced, hydrolyzed) by the reaction is called an *enzyme substrate,* and represents the species to be measured by the biosensor.

Widely used *enzymatic biosensors*[4,5] are being produced with multiple enzyme systems, to increase the number of measurable quantities (as the biosensor for the measurement of polyamine, using amino oxidase and peroxidase), as well as to amplify the reaction (as in the case of glucose oxidation by glucose-oxidase in the presence of glucose-reductase). The enzymatic biosensors provide a linear response for a wide range of substrate concentrations.

Antibodies. The antibodies (*Ab*) are glycoproteins produced by the immune system against specific external substances (antigens *Ag*). Theoretically it is possible to produce antibodies able to identify any antigen. Biosensors using antibodies as sensing elements are called *immunobiosensors.*[4,5]

Receptors. The regulation of biological processes at the molecular level is based upon specialized protein structures, called *receptors* (see Sec. 4.7.2), able to recognize a number of physiological signals. As an example, the neurotransmitter action is mediated by receptors present in the plasma membrane of the target cells; in this case the biologically active site can be an ionic channel. The acetylcholine receptor is the best known receptor in the field of neurotransmission (see Chaps. 4 and 11).

Cells and Tissues. The measurement of a molecular species, in some cases, requires not only its interaction with the biosensor molecule, but also its transformation (via biochemical reactions) into a measurable product. This could be done by using several enzymes with the appropriate cofactors; it is, however, simpler to operate with populations of cells where the metabolic pathway is naturally present. A relevant example of the complexity of the reactions at the surface of a biosensor caused by a population of bacteria is given by the *L-arginine* biosensor. In this case, bacterial cells of *Streptococcus faecium* are used in combination with an ammonia gas–sensing electrode. Arginine is assayed via the metabolism of arginine by the microorganisms, as shown in Fig. 10.3. It is difficult to obtain such complex reactions outside a cellular structure.

Instead of using a cell population as sensing element, it is possible to utilize slices of tissue (plant or animal); in this case there is the advantage of maintaining the cells in a natural environment, thus eliminating the danger of damaging them by trying to isolate them. For example, an *adenosine* biosensor,[4,5] has been proposed in which the biosensing

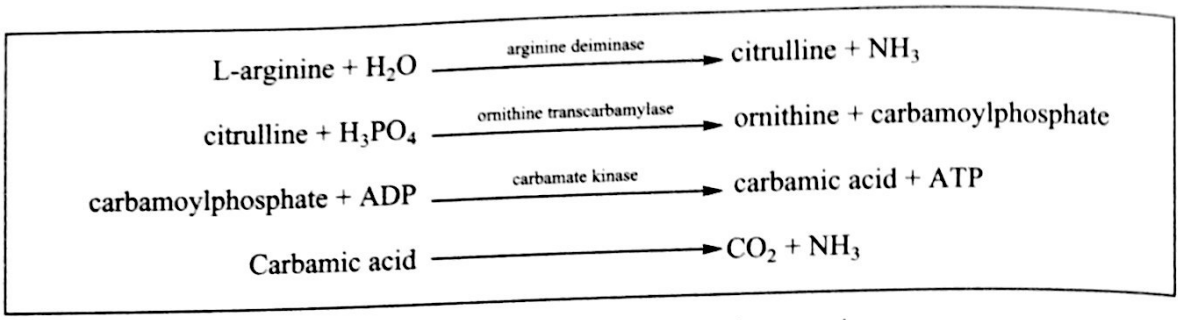

FIGURE 10.3 Metabolism of arginine by the microorganism sequence.

element is made of tissues obtained from mouse small-intestinal mucosal cells. Even the biocatalytic properties of the banana pulp have been used for *dopamine* sensing.[4,5]

10.1.2 Transducer

The transducer transforms the detection-induced physicochemical variations occurring in the biosensing element into a signal (usually electric), which is then amplified by an *ad hoc* designed electronic circuit and used in the control of external devices (such as an insulin pump). The transducer can be *electrochemical* (amperometric, potentiometric, conductometric), *optical, piezoelectric,* or *calorimetric.* Very often this classification is used to identify the type of biosensor.

Amperometric Biosensor. This is an electrochemical biosensor measuring the flux of electrons (current), generated by oxidation-reduction reactions induced by the biological component, toward a fixed-voltage electrode.[2,3] In these conditions the current is linearly dependent on the analyte concentration. The performance of these biosensors is directly related to the efficiency of electron transfer. This can be obtained with the use of redox molecules (*mediators*), such as *ferrocene,* placed on the electrode surface. The use of mediators reduces the possibility of interference on the oxidation-reduction processes caused by other analytes. The amperometric biosensor is characterized by its simplicity and its low implementation cost. This important advantage has lead to the introduction of disposable sensors, such as those for the measurement of blood glucose for diabetic patients ("reactive stripes"). The reactions on which this biosensor is based are schematically shown in Fig 10.4.

Potentiometric Biosensor. This is an electrochemical biosensor, operating at constant current (usually zero). It measures the charge-density variations on the electrode surface following a catalytic process or a surface modification due to the selective binding of a molecule.

A type of potentiometric biosensor consists of a modified MOSFET. Its operation is based on the interaction between H^+ ions (present in the solution) and the surface of the

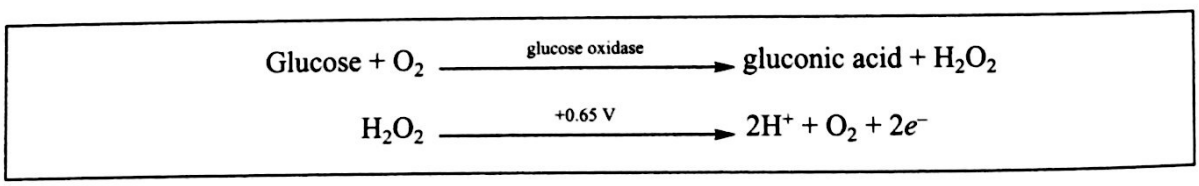

FIGURE 10.4 Reactions in an amperometric biosensor for the measurement of glucose concentration.

insulating layer (Si_3N_4, Al_2O_3, Ta_2O_5); such interaction induces a channel modulation in the transistor substrate.[1,3] On this principle, a simple pH-measuring device is based (see Sec. 7.1.4). Because of its robustness, miniaturization, and modularity, it can be employed where other more traditional pH meters cannot be used. This structure is the base of several enzymatic devices (ENFETs) designed to measure the pH variation caused by a reaction catalyzed by an enzyme, and consequently the substrate concentration.[7] Figure 10.5 shows the cross-section of the ENFET device, compared to the cross section of the traditional MOSFET.

Advantages of potentiometric biosensors based on MOS technology are related to their miniaturization, to their capability of measuring different species on the same silicon chip, and finally to the large-scale production capabilities of the microelectronic industry. Their major drawback consists in packaging difficulties.

Conductometric Biosensor. This is an electrochemical biosensor able to measure the electric conductivity of a solution, following the application (between two electrodes) of an electric field at a frequency of about 1 kHz. With these biosensors[4] it is possible to monitor the concentration changes of an ionic species or its migration velocity. An example is the measurement of urea via the urease enzyme. This enzyme decomposes the neutral substrate into ionic species, thus increasing the conductivity of the solution.

Optical Biosensor. This device is based on the emission, absorption, or scattering of light[5] and makes large use of optical fibers. Optical biosensors are comparable in dimensions to those based on MOS technology, but they do not require electrical contacts. The necessary instrumentation is, however, rather expensive. A relevant biosensor is the optical immunobiosensor, based on the evanescent wave phenomenon.[4]

Piezoelectric Biosensor. This contains a vibrating crystal, where the frequency of vibration is a function of the crystal mass.[4,5] The bond formation (direct or indirect, physical or chemical) between molecules and the crystal surface (e.g., due to their absorption or to the interaction with antibodies present on the crystal surface) produces a mass variation, which then induces a shift of the crystal resonance frequency. It can be used to measure gaseous pollutants with concentrations in the order of a few parts per billion.

Calorimetric Biosensor. The conductivity of this device has a high temperature coefficient, which allows the measurement of temperature variations in the order of millide-

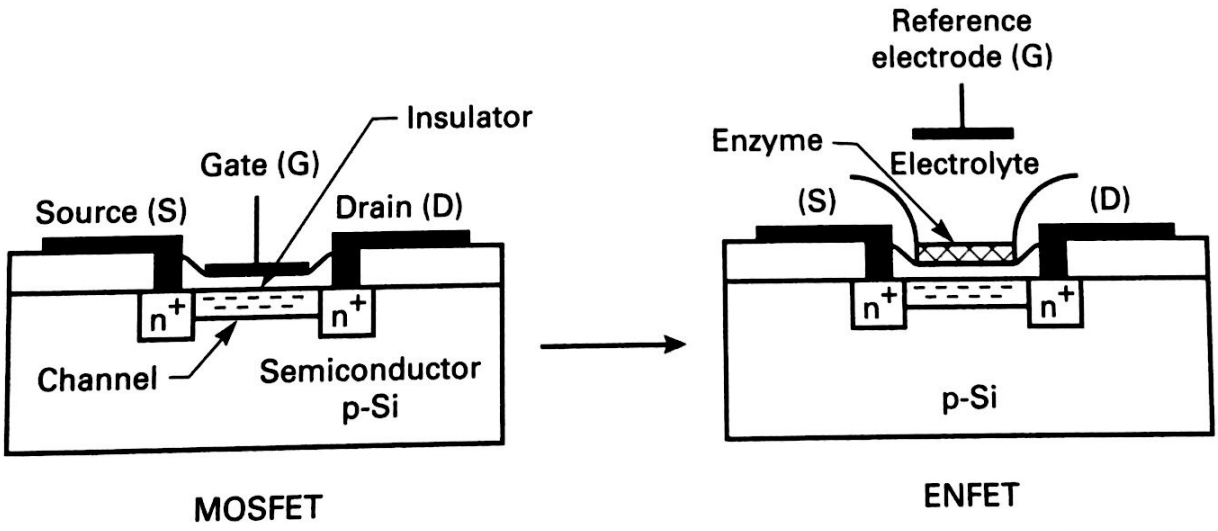

FIGURE 10.5 ENFET structure obtained by modification of the MOSFET structure. (*Kindly provided by Andrea Massobrio.*)

grees Celsius.[4] It is used to monitor fermentation processes, and can be coupled with enzymes, cells, and tissues.

10.1.3 Characteristics of Biosensors

The immobilization of the biosensing material represents a critical step in the production of biosensors, especially in dealing with enzymes and antibodies. A biosensor is specified by the following characteristics.

Selectivity. This is the capability to select and to measure only the desired biochemical species, with minimal interference from the many other species present in the environment. Just to give an example, it is not sufficient to use an antibody for which the desired species represents an antigen, because many antibodies can bind with other elements having on their surface the same functional group. It is very difficult to obtain total selectivity, not only of antibodies, but also of enzymes, microbic populations, and other biosensing elements.

Detection Limit. This defines the minimum concentration of the analyte to be measured, and determines the choice of certain types of biosensors when the analyte concentration values are very low.

Reversibility. To use a biosensor continously, it must be based on a reversible reaction. When the sensing element is an enzyme, its catalytic function makes it possible to return to the native form after the end of the chemical reaction. When using antibodies, the kinetics of the Ab-Ag binding is described by the affinity constant K_a = [AgAb]/[Ag][Ab], where [AgAb] is the concentration of the complex, and [Ag] and [Ab] are the concentrations of free antigen and antibody, respectively. Since the K_a value is usually very high (typical range 10^4 to 10^{12} M^{-1}), the Ab-Ag reaction is practically irreversible, and this puts some constraints to the design of immunobiosensors.

Lifetime. This parameter is related to the fact that the biosensing element can, with time, undergo degenerative processes, which cause the loss of the original biological function. A parameter which strongly influences the lifetime of the biosensor is related to the method of immobilization of the biosensing element, since some molecules may, with time, detach from the biosensor surface.

Response Time. The enzymatic or immunological reactions are characterized by fast kinetics; thus the response time of the biosensor is often not reaction-limited, but is rather diffusion-limited.

Biocompatibility. Some biosensors are designed to be used *in vivo;* since the introduction of a foreign element causes the body to start a response reaction, these biosensors have to use *biocompatible materials.* A widely used technique is to treat the surfaces with *albumin* (to reduce the contact between body and foreign material), and with *heparin* (to reduce the possibility of blood clot formation near the biosensor). As of today, there are no biosensors with good performances *in vivo,* and many efforts are devoted to solving this problem. In the case of glucose measurement (very important for diabetic people) promising results have been obtained with *ex vivo* systems.[8]

10.1.4 Applications of Biosensors

A way of classifying biosensor applications is according to the field in which the device is used.

1. *Clinical applications.* The diagnostic procedures are usually based on the measurements of species such as ions, gases, and hormones. Implantable biosensors can provide real-time measurements in critical conditions and drive feedback systems, in, for example, surgical operations.[9,10] It is thus possible to imagine that in the future the laboratory could be directly at bedside, in the home of the patient. Commercially available sensors include, for example, biosensors for (quick) tests for pregnancy, cholesterol, HDL, urine and blood glucose, and *Helicobacter* in the gastric mucose.
2. *Agriculture and horticulture.* In this area, biosensors show promising results in the measurement, in the field, of the degree of ripeness of several products.
3. *Industry.* Biosensors can be used as on-line monitors by canning and fermentation industries.[11]
4. *Environmental pollution.* In this field, biosensors can be used to monitor the presence of pesticides, herbicides, chemical fertilizers, and several water pollutants. Since on-line measurements are very important, the use of biosensors will probably represent a valuable early warning system.[12]
5. *Food quality.* In this field, biosensors are being used to monitor the presence of heavy metallic ions (e.g., Hg).[13]
6. *Defense.* Biosensors can be used in defense applications, to monitor the presence, for example, of nerve gases in the environment.

10.2 ION-SENSITIVE FIELD-EFFECT TRANSISTOR (ISFET)

As stated in the introduction of the chapter, and in accordance with the aim of the book, we will focus our attention now on a MOSFET-based biosensor.

The ion-sensitive field-effect transistor (ISFET), a device which measures pH or ions in solution, was reported first by Bergveld.[14] The structure of the ISFET, as shown in Fig. 10.6, is fundamentally a MOSFET, the essentials of which are given in Chaps. 8 and 9, which can be rendered H^+-sensitive by eliminating its metal gate electrode in order to expose the gate insulator to the solution. The introduction of an ion-selective membrane can make it sensitive to other specific ions.

The ISFET, in its basic form, is a potentiometric pH electrode. Therefore, strictly speaking, it is not a biosensor, but rather a chemical sensor, which can be compared with the traditional pH-glass membrane electrode, based on the Nernst potential. The ISFET advantages are planar construction, small dimensions, low impedance, fast response, large-scale production, ease of multisensor (differential) realization, and immediate use after dry storage. A drawback is the larger drift rate and the necessary stringent encapsulation of the chip edges and bonding leads. In the next section, the ISFET will be used as the basis of potentiometric enzyme sensors (ENFET).[7]

The gate insulator of the ISFET senses the H^+ ion concentration, generating an interface potential on the gate; the corresponding drain-source current change in the semiconductor channel is observed. From a comparison of the MOSFET and ISFET structures, it is apparent that the only difference between the electrical circuits is the replacement of the

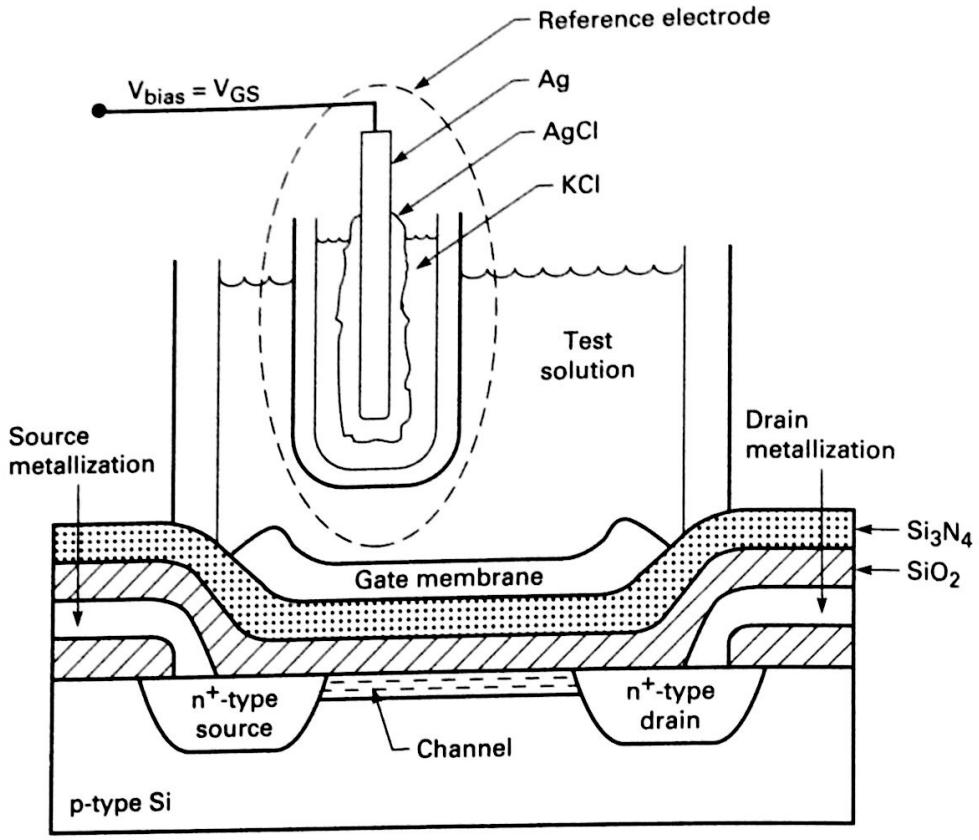

(a)

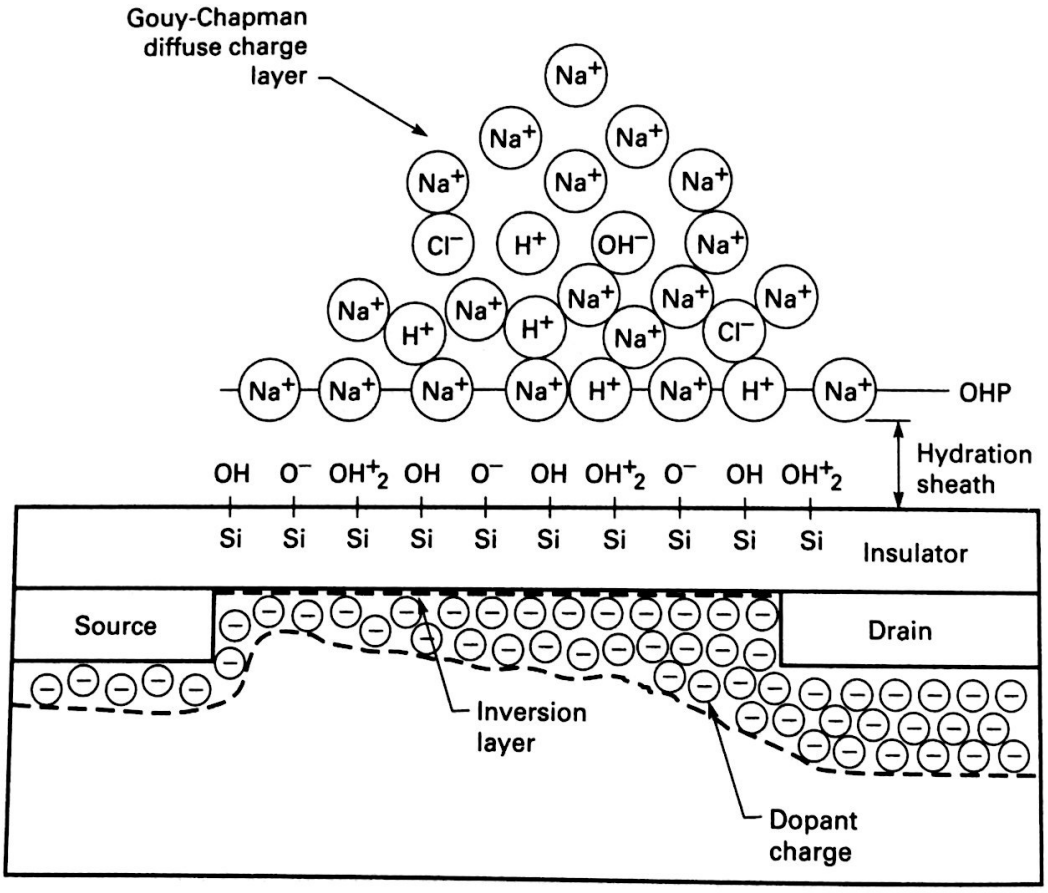

(b)

FIGURE 10.6 (*a*) Schematic representation of an ISFET; where a gate membrane is also shown; (*b*) expanded view of semiconductor-insulator-electrolyte interface (SiO_2 indicated for simplicity).

metal gate of the MOSFET by the series combination of a reference electrode, electrolyte solution, and a chemically sensitive insulator. The reference electrode provides a stable potential (see Sec. 7.1.1) in the solution independent of changes in the dissolved species or in the pH of the solution. The gate voltage is applied to the reference electrode to produce the channel in the semiconductor.

As already stated, the operational mechanism of the ISFET originates from the pH sensitivity of the inorganic gate oxide, such as SiO_2, Al_2O_3, Si_3N_4, or Ta_2O_5. This mechanism is a surface phenomenon which can be explained by the site dissociation model (see Sec. 7.1.4).

Surface hydroxyl groups react with the analyte in an acidic or a basic way, resulting in a corresponding surface charge and potential. Depending on the specific properties of the gate oxide, this surface potential is in the order of 25 mV/pH (SiO_2) to 59 mV/pH (Ta_2O_5). The response is determined by the kinetics of the surface reactions, and response times in the order of milliseconds are typical. It should be pointed out that the potential drop at the solid-liquid junction is influenced by the properties of the solid material, which can change over time, giving rise to apparently "nonnernstian" responses.

The temperature sensitivity of the ISFET is mainly determined by the semiconductor component of the sensor. A method to compensate for this temperature sensitivity is to use a differential pair of ISFETs or an ISFET and a MOSFET, as in electronic systems. Since the ISFET is an open transistor, it is also sensitive to light, but this can also be compensated for by the application of a differential pair.

The requirement of the reference electrode is difficult to meet by using integrated circuit technology to build it on a silicon chip. A reference electrode uses a chemical reaction to move ions into solution from an electrode. For example, with the Ag/AgCl reference electrode, the motion of chloride ions from or to the solid Ag/AgCl electrode carries the current

$$e^- + AgCl \rightleftharpoons Ag + Cl^- \tag{10.1}$$

The Nernst equation for the potential with such a reaction is

$$V = V_o - (RT/\mathcal{F}) \ln [Cl^-] \tag{10.2}$$

where V is the potential of the Ag electrode, V_o a constant, R the gas constant (see App. A), $\mathcal{F}$ the Faraday constant (see App. A), T the absolute temperature, and $[Cl^-]$ the concentration of chloride ions. If there is a constant concentration of chloride ions, the potential V is stable, as desired. Such a stable concentration can be easily obtained with a typical reference electrode where the Ag/AgCl is isolated from the solution to be tested by a frit (or a salt bridge) and KCl is provided on the Ag/AgCl side of the frit. This is not so easy to obtain if the reference electrode is, for example, a silver film deposited on a silicon chip for compatability with FET technology.[3]

In this section we have given a qualitative overview of the ISFET; in the next sections we will present a quantitative description of the device operation mechanisms.

10.2.1 ISFET Operation

All chemical sensors based on the field-effect operation share a common feature. Their measurable properties can be described in terms of the flat-band potential V_{FB}. As we have seen, the threshold voltage, V_{TH} is directly related to V_{FB} [Eq. (8.36)]. In the following, we show how we can make V_{FB}, and consequently V_{TH} and I_{DS}, sensitive to different chemical entities in the medium contacting the sensor.

Then let us consider a system consisting of the following components: a reference electrode, which contains a stable solid-liquid interface, an electrolyte, an insulating layer

(eventually consisting of layers of different insulators), a silicon substrate, and a metal back contact. In the usual electrochemical representation, this system is written as

M | Si | Insulator | Electrolyte | Reference electrode | M′

The most important measurable parameter of this system is its flat-band voltage V_{FB}, defined as the voltage applied to M′ which makes the silicon surface potential zero. In Ref. 15 it is shown that

$$V_{FB} = (E_{ref} + \varphi_{lj}) - (\varphi_{eo} - \chi_e) - \frac{\phi_{Si}}{q} - \frac{Q_o}{C_{ox}} \tag{10.3}$$

where E_{ref} is the reference electrode potential relative to vacuum, which is obtained by adding 4.7 V to the potential relative to the normalized hydrogen electrode; φ_{lj} is the liquid-junction potential difference between the reference solution and the electrolyte; φ_{eo} is the potential drop in the electrolyte at the insulator-electrolyte interface; χ_e is the surface dipole potential of the solution; ϕ_{Si} is the work function of Si; C_{ox} and Q_0 are the insulator capacitance and effective charge per unit area (see Sec. 8.6).

In the expression of V_{FB} of the MOSFET, the terms in parenthesis are replaced by the work function of the contacting metal [ϕ_{MS}; see Eq. (8.36)]. Thus, the flat-band voltage, and therefore the threshold voltage, is the quantity measured in chemically sensitive electronic devices based on the field-effect principle. Taking into account Eqs. (8.36), (8.37), and (10.3), we can write

$$V_{TH}(\text{ISFET}) = V_{TH}(\text{MOSFET}) + E_{ref} + \varphi_{lj} + \chi_e - \varphi_{eo} - \frac{\phi_M}{q} \tag{10.4}$$

where ϕ_M is the work function of the metal back contact of the semiconductor relative to vacuum. Equation (10.4) replaces the MOSFET threshold voltage in the I_{DS}-V_{DS} equations [see Eqs. (9.15) and (9.19)]. The main source of the pH sensitivity of the ISFET, among the terms in Eq. (10.3), is the potential drop φ_{eo} in the electrolyte at the insulator-electrolyte interface.

On the basis of site-binding theory,[16] applied to the amphoteric metal oxide gate materials used in ISFETs, the sensitivity of this device is described in terms of the intrinsic buffer capacity of the oxide surface, β_s, and the electrical surface differential capacitance C_s. The ISFET sensitivity toward changes in the bulk pH is described by the ratio β_s/C_s.

An approach, originally proposed by Bergveld and coworkers,[17] to the description of the acid-base properties of ISFETs is analogous to the classical description of the acid-base properties of protein molecules (see Chap. 4). The acid-base titration of proteins is also determined by the ratio between the intrinsic buffer capacity and the electrical double-layer capacitance.

The conclusion that ISFET surfaces and protein molecules behave in a similar way with respect to their acid-base properties is an alternative description of the operational mechanism of the ISFET, and it is simpler and more easily understood than the original theory,[18] which will be used in Chap. 12.

10.2.2 pH Dependency of φ_{eo}: A Measure of the pH Sensitivity of the ISFET

The origin of the potential φ_{eo} is the interaction of the insulator surface with ions present in the electrolyte. The main feature of all theories for this interaction is that the presence of discrete surface sites is assumed. The model used can have one or more different types

of sites, each with acidic, basic, or amphoteric character. For the Al_2O_3 oxide which we will take into account (the use of insulator Si_3N_4 is considered in Chaps. 7 and 12), it is usual to consider that only one type of site is present, of the type A-OH, where A represents Al.[18] To account for the fact that both signs of charge have been experimentally observed in colloid chemical studies, the site considered must be amphoteric, which means it can act as a proton donor or acceptor. We then assume that the oxide surface contains sites in three possible forms: $A\text{-}O^-$, A-OH, and $A\text{-}OH_2^+$. The acidic and basic character of the neutral site A-OH can be characterized by two equilibrium constants K_a and K_b (acidity and basicity constants, respectively):

$$A\text{-}OH \rightleftharpoons A\text{-}O^- + H_s^+ \qquad \text{with } K_a = \frac{[A\text{-}O^-][H^+]_s}{[A\text{-}OH]} \tag{10.5}$$

$$A\text{-}OH + H_s^+ \rightleftharpoons A\text{-}OH_2^+ \qquad \text{with } K_b = \frac{[A\text{-}OH_2^+]}{[A\text{-}OH][H^+]_s} \tag{10.6}$$

In Eqs. (10.5) and (10.6), [A-OH] is the surface concentration of neutral sites, and $[A\text{-}O^-]$ and $[A\text{-}OH_2^+]$ the surface concentration of negative and positive surface sites respectively, the values of which are given by the respective equilibrium constants and the pH of the bulk solution, pH_b. The quantity $[H^+]_s$ indicates the volume concentration of protonated water molecules, $[H_3O^+]$, in contact with the oxide surface, the value of which can be obtained by combining Eqs. (10.5) and (10.6), i.e.,

$$[H^+]_s = \sqrt{\frac{K_a}{K_b}\frac{[A\text{-}OH_2^+]}{[A\text{-}O^-]}} \tag{10.7}$$

Equation (10.7), for the neutral surface—that is, when $[A\text{-}OH_2^+] = [A\text{-}O^-]$—reduces to

$$[H^+]_s = \sqrt{\frac{K_a}{K_b}} \tag{10.8}$$

or, equivalently, we can write

$$pH_s = -\log[H^+]_s = -\log\sqrt{\frac{K_a}{K_b}} \tag{10.9}$$

This neutral equilibrium situation is established for a value where $pH_b = pH_s$, which is generally known as the pH at the *point of zero charge* (pH_{pzc}), which is characteristic of a certain type of oxide (see Sec. 7.1.4). When the surface is in contact with an electrolyte with a value of $pH_b \neq pH_{pzc}$, the effect on pH_x can be expressed in terms of the *intrinsic buffer capacity of the surface,* β_s (see Sec. 4.2.2), which is by definition the ratio between a small amount of strong base d[B] (or acid) concentration added to the solution and the resulting change in pH, indicated as dpH_s, i.e.,

$$\beta_s = \frac{d[B]}{dpH_s} \tag{10.10}$$

The sign of Eq. (10.10) is correct if OH^- ions are considered, otherwise, if H^+ ions are considered, the sign must be changed. Therefore,

$$[B] = [A\text{-}O^-] - [A\text{-}OH_2^+] = -\frac{\sigma_s}{q} \tag{10.11}$$

where σ_s is the net surface concentration charge of the titrated groups and q is the electronic charge.

Considering the total concentration of charged and neutral surface sites

$$N_s = [\text{A-O}^-] + [\text{A-OH}_2^+] + [\text{A-OH}] \tag{10.12}$$

we can calculate, from Eqs. (10.5), (10.6), and (10.12), the concentration of the negative and positive surface concentration sites, as

$$[\text{A-OH}^+] = N_s \frac{K_a}{K_a + [\text{H}^+]_s + K_b[\text{H}^+]_s^2} \tag{10.13}$$

and

$$[\text{A-OH}_2^+] = N_s \frac{K_b[\text{H}^+]_s^2}{K_a + [\text{H}^+]_s + K_b[\text{H}^+]_s^2} \tag{10.14}$$

Thus, Eqs. (10.10) and (10.11) give[17]

$$\beta_s = \frac{d[\text{B}]}{d\text{pH}_s} = \frac{d[\text{B}]}{d[\text{H}^+]_s} \cdot \frac{d[\text{H}^+]_s}{d\text{pH}_s}$$

$$= N_s \frac{K_a + 4K_aK_b[\text{H}^+]_s + K_b[\text{H}^+]_s^2}{(K_a + [\text{H}^+]_s + K_b[\text{H}^+]_s^2)^2} \cdot 2.3[\text{H}^+]_s \tag{10.15}$$

Equation (10.15) indicates that the buffer capacity of an amphoteric surface becomes larger with a larger value of N_s, as well as with a larger value of the product K_aK_b, which is equivalent to considering a small value of $\Delta pK = (pK_a + pK_b)$.

Because of the intrinsic buffer capacity of the surface, the value of pH_s does not follow the value of pH_b during titration, and this gives rise to a surface potential φ_{eo}, according to the Boltzmann distribution

$$[\text{H}^+]_s = [\text{H}^+]_b e^{-q\varphi_{eo}/kT} \tag{10.16}$$

or, equivalently,

$$\varphi_{eo} = 2.3 \frac{kT}{q} (\text{pH}_s - \text{pH}_b) \tag{10.17}$$

According to the derivation given in Sec. 7.2.1, the charge in the diffuse layer can be written as

$$\sigma_d = -(8kT\varepsilon_0\varepsilon_r c_0)^{1/2} \sinh\left(\frac{zq\varphi_{eo}}{2kT}\right) = -\sigma_s \tag{10.18}$$

where c_0 is the ion concentration in the bulk and z is the ion valence. Equation (10.18) indicates the integral capacitance of the system which will be further considered in Sec. 10.3.4 when the response of the ISFET to stepwise changes in the ionic strength, will be considered.

The ability of the electrolyte to store charge in response to a change in the electrostatic potential is the differential capacitance

$$\frac{d\sigma_d}{d\varphi_{eo}} = -\frac{d\sigma_s}{d\varphi_{eo}} = -C_s \tag{10.19}$$

A complete expression of the charge balance should include the charge in the semiconductor component. In this treatment, this contribution will be neglected; it will be taken into account in Chap. 12.

A change with the bulk pH_b induces a change in pH_s, which in turn results in a change in the surface potential φ_{eo}.

According to Eqs. (10.10), (10.11), and (10.19), we can write

$$\frac{d\varphi_{eo}}{d\mathrm{pH}_s} = \frac{d\sigma_s}{d\mathrm{pH}_s}\frac{d\varphi_{eo}}{d\sigma_s} = -\frac{q\beta_s}{C_s} \tag{10.20}$$

under the condition that C_s is independent of φ_{eo}, which is in most cases a reasonable assumption,[17] and taking into account the convention on the sign for β_s.

Equation (10.20) indicates that for a small value of $d\mathrm{pH}_s$, a large value of $d\varphi_{eo}$ will take place when the surface has a large intrinsic buffer capacity β_s, especially in combination with a small electrical surface capacitance C_s.

Since an ISFET is a device that measures the gate insulator-electrolyte interface potential φ_{eo}, as a function of the pH of the bulk electrolyte pH_b, Eq. (10.17) must be differentiated to determine the pH sensitivity of the ISFET, i.e.,

$$\begin{aligned}\frac{d\varphi_{eo}}{d\mathrm{pH}_b} &= 2.3\frac{kT}{q}\left(\frac{d\mathrm{pH}_s}{d\mathrm{pH}_b} - 1\right)\\ &= 2.3\frac{kT}{q}\left(\frac{d\mathrm{pH}_s}{d\varphi_{eo}}\frac{d\varphi_{eo}}{d\mathrm{pH}_b} - 1\right)\end{aligned} \tag{10.21}$$

Rearranging Eq. (10.21) yields

$$\frac{d\varphi_{eo}}{d\mathrm{pH}_b} = \frac{2.3\dfrac{kT}{q}}{2.3\dfrac{kT}{q}\dfrac{d\mathrm{pH}_s}{d\varphi_{eo}} - 1} \tag{10.22}$$

Combining Eqs. (10.20) and (10.22), we obtain

$$\frac{d\varphi_{eo}}{d\mathrm{pH}_b} = -2.3\frac{kT}{q}\frac{1}{2.3\dfrac{kT}{q^2}\dfrac{C_s}{\beta_s} + 1} = -2.3\alpha\frac{kT}{q} \tag{10.23}$$

where

$$\alpha = \frac{1}{2.3\dfrac{kT}{q^2}\dfrac{C_s}{\beta_s} + 1} \tag{10.24}$$

is a dimensionless sensitivity parameter which varies between 0 and 1 depending on the intrinsic buffer capacity and the differential capacitance.

The pH sensitivity of an ISFET with an inorganic oxide as the gate material can then be described through the parameter α, which approaches unity for large values of β_s/C_s. This means that surfaces with a large buffer capacity (large value of N_s and low value of ΔpK) and a low value of C_s (low electrolyte concentration) show at best a maximum response of 59.3 mV at 25°C.[17] This value is achieved by oxides with a large intrinsic buffer capacity, such as Ta_2O_5. On the other hand, an oxide such as SiO_2 exhibits a low pH sensitivity.

10.3 ENZYME FIELD-EFFECT TRANSISTOR (ENFET)

The enzyme field-effect transistor (ENFET) is a bioelectronic device which belongs to a class of chemical potentiometric sensors that take advantage of the high selectivity and sensitivity of biologically active materials (here enzymes). In these devices, the enzyme is immobilized on the insulator of the ISFET. In literature, a dual-gate ISFET is often proposed, where one of the FETs can act as a reference system and is assembled in the same way as the sample FET, but it contains a blank enzyme-free gel membrane (Fig. 10.7). This arrangement allows some automatic compensation of fluctuations in solution pH and temperature.

The enzyme-substrate system controls the specificity of the ENFET operation, and the reaction kinetics that take place in the biologically active materials (enzyme) determine how fast the substrate is converted into the product. To get an understanding of the ENFET operation, the reaction kinetics of the biological-recognition processes must be considered, together with the mass transport theory (Fig. 10.8).

A detailed discussion, however, is beyond the aim of this chapter; in addition, solutions to the transport equations for ENFET structures need a detailed knowledge of the diffusion coefficients for all species involved in the reactions and the geometry of the sensor structure. In addition, the partial differential equations usually require numerical solutions.

10.3.1 System Definition

Consider the system consisting of a sensor surface, lying at $x = 0$, coated with an immobilized enzyme layer of thickness L. Beyond this lies the transport boundary layer. Beyond the transport boundary layer, the concentration of analyte, the enzyme's substrate S, has a defined value [S] and that of the product [P] is taken to be zero (see Fig. 10.9). Notice that these bulk concentrations of substrate and product represent two basic boundary conditions of the system. Enzyme-catalyzed reaction takes place in the immobilized enzyme layer and, for the present description, will be considered to follow Michaelis-Menten kinetics (see Sec. 5.4.2). This reaction depletes the substrate and gen-

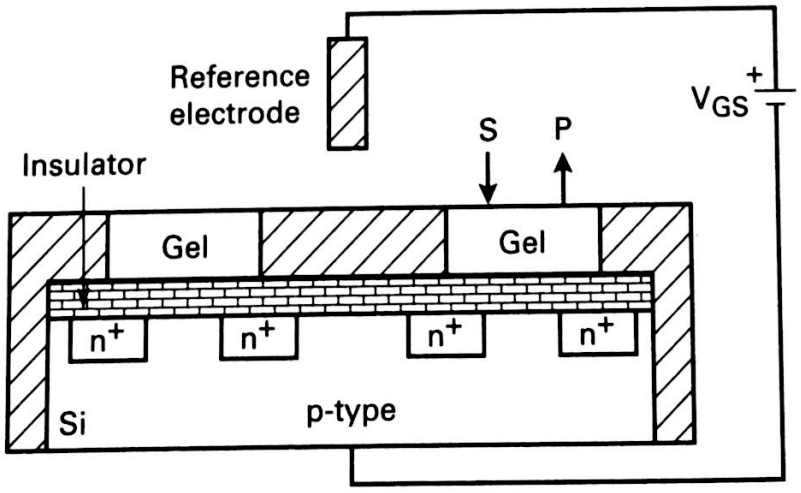

FIGURE 10.7 Schematic representation of a dual-gate ENFET chip. (*From S. D. Caras and J. Janata.*[19])

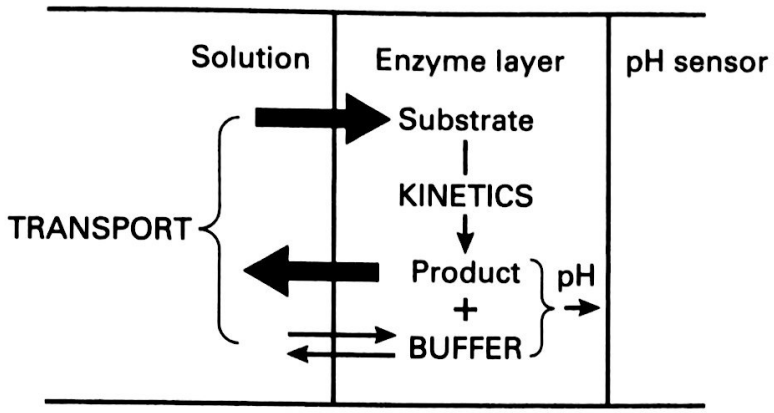

FIGURE 10.8 Mechanisms involved in the response of pH-based enzyme sensors. (*From B. H. van der Schoot and P. Bergveld.*[7])

erates the product in the enzyme layer, causing the concentration gradients which drive the mass transport process. The product is measured potentiometrically, without being consumed, at the sensor surface. A steady state is reached when the rate of reaction in the immobilized enzyme layer is balanced by mass transport of reactant and product to and from it.

10.3.2 Enzyme-Catalyzed Reaction of Substrate

For the sake of self-consistency and for readers' convenience, some concepts already introduced in Chap. 5, will be considered here again. Note that here, the enzyme is assumed to be immobilized in a region of space, and then mass transfer mechanisms (in particular diffusion) must be taken into account.

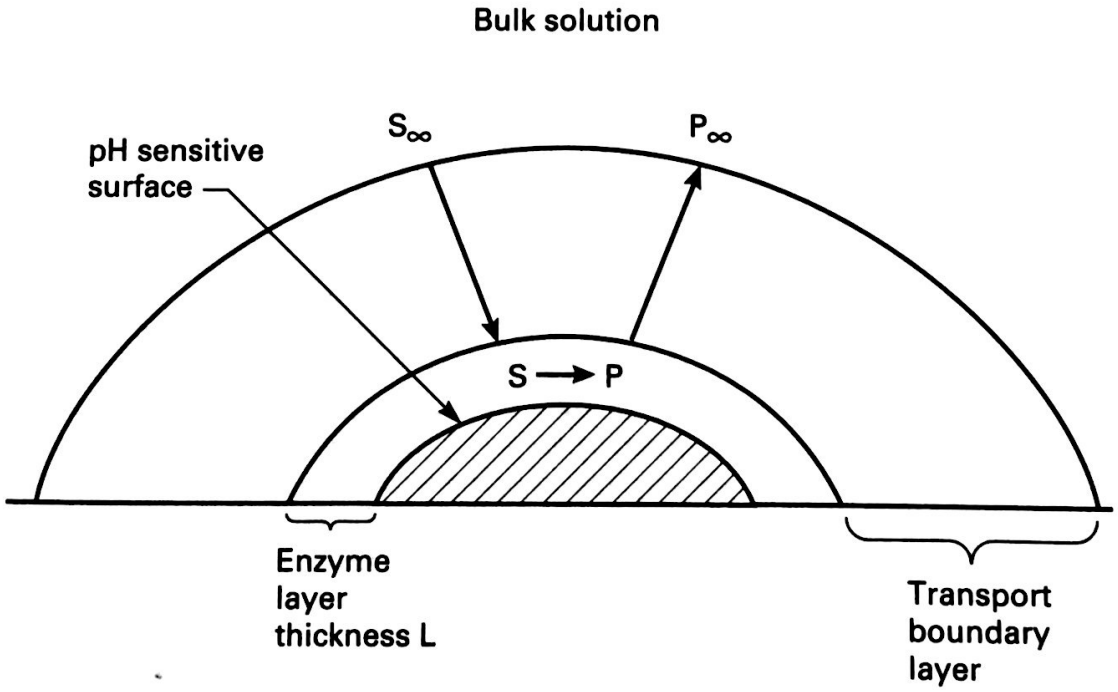

FIGURE 10.9 Schematic representation of the potentiometric biosensor using an immobilized enzyme layer.

Let us consider a single enzyme acting on a substrate molecule, where any other reactants are assumed to be in excess so as not to limit the reaction. The reaction then follows the Michaelis-Menten kinetics (see Sec. 5.4.2)

$$S + E \underset{k_{-1}}{\overset{k_1}{\rightleftharpoons}} ES \xrightarrow{k_2} P + E \tag{10.25}$$

where E is the enzyme, S is the substrate, ES is the bound intermediate enzyme-substrate complex (indicated as C in Sec. 5.4.2), P is the product and k_1, k_{-1}, k_2 are the reaction-rate constants for the enzyme-substrate binding (forward) reaction, the unbinding (backward) of the enzyme-substrate complex, and the formation of the product (or complex decomposition), respectively.

The rate of product formation is given by

$$v_f = \frac{\partial[P]}{\partial t} = k_2[ES] \tag{10.26}$$

where the rate v_f has units of mol/l-s and t is the time. To relate the rate of product formation with the substrate concentration, it is assumed that the reaction is in steady state; that is, by assuming that the rates of formation and breakdown of the complex are equal. This assumption, which is valid almost immediately after the reaction has begun, leads us to write the rate equation for the intermediate complex as

$$\frac{\partial[ES]}{\partial t} = k_1[E][S] - k_{-1}[ES] - k_2[ES] = 0 \tag{10.27}$$

Since the total concentration of enzyme $[E]_o$ present at all times will be the sum of concentrations in free and complexed forms [E] + [ES], we substitute $[E] = [E]_o - [ES]$ into Eq. (10.27), solve it for [ES], and substitute into Eq. (10.26), obtaining

$$v_f = \frac{k_2[ES]_o[S]}{([S] + K_M)} = k_2[ES] \tag{10.28}$$

where we have introduced the Michaelis constant defined as

$$K_M \equiv \frac{(k_{-1} + k_2)}{k_1} \tag{10.29}$$

The Michaelis constant K_M is not a true equilibrium constant but is the ratio of rate constants for complex formation and disappearance, the latter comprising both simple dissociation back to reactants plus decomposition into products.

Few enzymes follow the Michaelis-Menten kinetics over a wide range of experimental conditions. Most enzyme-substrate interactions have more complex kinetics, for example, the reverse reaction in which complex formation between the enzyme and product must be taken into account, multiple substrates with additional reaction steps, and inhibition. However, for these cases with complex kinetics, K_M is still a useful measure of the enzyme-substrate interaction.

When the enzyme is brought in contact with a substrate (glucose, for example), a complex concentration profile develops, which is a function of both diffusion and reaction processes. In the reaction region of the enzyme, the product concentration is achieved by mass transfer given by Fick's second law as well as by enzyme kinetics. The mass transport has been discussed in Sec. 5.1.

10.3.3 Enzyme-Modified Ion-Sensitive Field-Effect Transistor (ENFET)

For a gel membrane-immobilized system, the coupled mass transport and kinetic reaction for the depletion of substrate across the gel layer must be considered.

The enzyme reaction rate follows the Michaelis-Menten kinetics, Eq. (10.25), and the concentration of the substrate and the product in the enzyme membrane are described by the diffusion-reaction equation, which is just Fick's second law with a term added to account for the consumption or production of a species,[19] i.e.,

$$\frac{\partial C}{\partial t} = D\frac{\partial^2 C}{\partial x^2} \pm R(C) \tag{10.30}$$

where D is the diffusion coefficient of the species, $R(C)$ is the reaction term, and the sign depends on whether species is produced (product) or consumed (substrate). Considering the steady-state response, the time derivative will be set to zero. Using the Michaelis-Menten kinetics, Eq. (10.28), as the reaction term, Eq. (10.30) becomes, for the *substrate,*

$$D_S\frac{\partial^2[\mathrm{S}]}{\partial x^2} - \frac{k_2[\mathrm{E}]_o[\mathrm{S}]}{K_M + [\mathrm{S}]} = 0 \tag{10.31}$$

and for the *product,*

$$D_P\frac{\partial^2[\mathrm{P}]}{\partial x^2} + \frac{k_2[\mathrm{E}]_o[\mathrm{S}]}{K_M + [\mathrm{S}]} = 0 \tag{10.32}$$

where D_S and D_P are the diffusion coefficients of the substrate in the gel layer and of the product, respectively.

An exact solution to Eqs. (10.31) and (10.32) needs numerical techniques. However, analytical solutions can be found when we consider the two limiting cases, $[\mathrm{S}] \ll K_M$ and $[\mathrm{S}] \gg K_M$. The first case represents enzyme kinetics that are much faster than the transport through the membrane, the substrate concentration being the limiting factor. The second case accounts for very high substrate concentration that saturates the enzyme.

In the first limiting case, $[\mathrm{S}] \ll K_M$, Eq. (10.31) becomes

$$\frac{\partial^2[\mathrm{S}]}{\partial x^2} - \alpha[\mathrm{S}] = 0 \tag{10.33}$$

where

$$\alpha = \frac{k_2[\mathrm{E}]_o}{K_M D_S} \tag{10.34}$$

is the *enzyme loading factor* or *diffusion modulus,* which represents the effective concentration of the enzyme, including the concentration of enzyme in the membrane, the kinetics of the enzyme reaction, and the mass transport (diffusion) of the substrate molecules through the membrane. The boundary conditions we use to solve Eq. (10.33) are

$$\left.\frac{\partial[\mathrm{S}]}{\partial x}\right|_{x=0} = 0 \tag{10.35a}$$

$$[\mathrm{S}]|_{x=L} = [\mathrm{S}]_L \tag{10.35b}$$

where $[\mathrm{S}]_L$ is the substrate concentration at the outer surface of the immobilized enzyme layer at $x = L$.

The physical meaning of Eqs. (10.35) is that, at the transducer's surface ($x = 0$), there is no transport flux (the substrate is neither consumed nor generated there, so that with no reaction at the surface, there can be no reaction flux), and at the outer edge of the membrane ($x = L$), the substrate concentration is fixed at the value of the analyte solution at the membrane's outer surface. The solution for the substrate concentration is[20–22]

$$[\mathrm{S}] = \left(\frac{\cosh (x\sqrt{\alpha})}{\cosh (L\sqrt{\alpha})} \right) [\mathrm{S}]_L \tag{10.36}$$

where x defines the distance across the gel-membrane layer, which extends from the interface between the gel and the transducer's surface at $x = 0$, to the gel-solution interface at $x = L$. The term we are interested in is the product concentration at the transducer's surface ($x = 0$). To find a relationship of product concentration from the substrate concentration, we add Eqs. (10.31) and (10.32), i.e.,[20–22]

$$D_S \frac{\partial^2 [\mathrm{S}]}{\partial x^2} + D_P \frac{\partial^2 [\mathrm{P}]}{\partial x^2} = 0 \tag{10.37}$$

In this way the kinetic term due to the enzyme catalyzed reaction disappeared. Equation (10.37) can be integrated once to give

$$D_S \frac{\partial [\mathrm{S}]}{\partial x} + D_P \frac{\partial [\mathrm{P}]}{\partial x} = \text{constant} \tag{10.38}$$

Equation (10.38) represents the diffusion fluxes in the enzyme layer. At the membrane's outer surface ($x = L$), the product and substrate fluxes must balance in the steady state, since no material is being created or destroyed. Thus, the value of the constant must be zero throughout the membrane. Integrating Eq. (10.38) between $x = 0$ and $x = L$, results in the mass balance equation for the membrane:

$$D_S[\mathrm{S}]_L + D_P[\mathrm{P}]_L = D_S[\mathrm{S}] + D_P[\mathrm{P}] = \text{constant} \tag{10.39}$$

Combining Eq. (10.39) and Eq. (10.36), and solving for [P], we obtain[20–22]

$$[\mathrm{P}] = \frac{D_S}{D_P} \left[1 - \frac{\cosh (x\sqrt{\alpha})}{\cosh (L\sqrt{\alpha})} \right] [\mathrm{S}]_L + [\mathrm{P}]_L \tag{10.40}$$

Setting $x = 0$ in Eq. (10.40) gives the surface concentration of product, which is proportional to the transducer's output signal in an ENFET, in terms of the substrate concentration in the solution

$$[\mathrm{P}]|_{x=0} = \frac{D_S}{D_P} \left(1 - \frac{1}{\cosh (L\sqrt{\alpha})} \right) [\mathrm{S}]_L + [\mathrm{P}]_L \tag{10.41}$$

Equation (10.41) indicates that, for the limiting case $K_M \gg [\mathrm{S}]_L$, the surface concentration is directly proportional to the substrate concentration at the enzyme layer outer surface. This description of the system involves the parameter $L\sqrt{\alpha}$, which includes the important kinetic variables of the system.

Equation (10.41) shows that there is a term for the concentration of product just outside the membrane. This term can derive from the slow diffusion of the product into the bulk solution or from the presence of the product as part of the solution.

In the second limiting case, $[S] \gg K_M$, Eqs. (10.31) and (10.32) become

$$D_S \frac{\partial^2[S]}{\partial x^2} - k_2[E]_o = 0 \tag{10.42}$$

and

$$D_P \frac{\partial^2[P]}{\partial x^2} + k_2[E]_o = 0 \tag{10.43}$$

Equations (10.42) and (10.43) can be integrated, and both are subject to the boundary conditions of Eqs. (10.35). The solution for the substrate concentration is then

$$[S] = [S]_L + \frac{k_2[E]_o}{2D_S}(x^2 - L^2) \tag{10.44}$$

and for the product concentration

$$[P] = [P]_L + \frac{k_2[E]_o}{2D_P}(L^2 - x^2) \tag{10.45}$$

From Eq. (10.45), we can notice that the product concentration at the surface ($x = 0$) of the transducer is a constant that depends on the immobilized enzyme concentration, the reaction kinetics, the diffusion mass transport, and it is independent of substrate concentration. Therefore the output of the biosensor is constant. In this case the substrate concentration is so large that it has saturated the enzyme. Then there is no sufficient amount of enzyme in the membrane to detect changes in such a large substrate concentration.

The above analysis shows that, for a given amount of enzyme in the membrane, the response of the sensor will go from an approximately linear dependence on the analyte concentration to a saturation value for an increase of the analyte concentration. We remind the reader that the above analysis has been performed in absence of buffer. In practice, a buffer is always present and the introduction of feedback can take care of it.[7]

Analytical solutions of the differential equations written above, are described in detail in Ref. 22.

We now consider the response of an ISFET, modified by an immobilized enzyme layer E that catalyzes the reaction of the substrate S, leading to formation of the acid HA/($H^+ + A^-$), according to the reaction

$$S \xrightarrow{E} HA \rightleftharpoons H^+ + A^- \tag{10.46}$$

In the steady state, a balance between the rates of mass transport of the substrate from bulk solution to the enzyme layer, production of the acid by the enzyme layer and transport of the product acid into the bulk solution will be achieved, leading to a stable local pH change in the region of the immobilized enzyme layer.

The mass transport of product acid from the surface of the immobilized enzyme layer into bulk solution is a complex problem because of proton association and dissociation reactions in solution. First, the proton dissociation and association reactions of the acid itself must be taken into account, i.e.,

$$H^+ + A^- \underset{k_{-a}}{\overset{k_a}{\rightleftharpoons}} HA \tag{10.47}$$

Second, the reaction of any buffer system, B^-/BH, must be considered, i.e.,

$$H^+ + B^- \underset{k_{-b}}{\overset{k_b}{\rightleftharpoons}} HB \tag{10.48}$$

Complete analytical solution of the set of differential equations describing mass transport coupled with the kinetics of acid protonation and deprotonation reactions is not possible, either in the presence or absence of buffer.

Concentration profiles for the involved species across the enzyme layer, and in particular the H^+ concentration at the pH-sensitive surface can be derived by adding to Eq. (10.31) the following relations[23]

$$D_{H+}\frac{\partial^2[H^+]}{\partial x^2} + \frac{k_2[E]_o[S]}{K_M + [S]} - k_b[B^-][H^+] + k_{-b}[BH] = 0 \tag{10.49}$$

$$D_{BH}\frac{\partial^2[BH]}{\partial x^2} + k_b[B^-][H^+] - k_{-b}[BH] = 0 \tag{10.50}$$

$$D_{B-}\frac{\partial^2[B^-]}{\partial x^2} - k_b[B^-][H^+] + k_{-b}[BH] = 0 \tag{10.51}$$

where D = diffusion coefficients of the various species in the immobilized enzyme layer
k_2 and K_M = constants for Michaelis-Menten enzyme kinetics as previously described
[E] = enzyme concentration in the immobilized layer
k_b and k_{-b} = forward and backward rate constants for the buffer protonation reaction

Solution of these equations with suitable boundary limits gives a model for the response of an enzyme-modified ISFET in buffer solution. For further details, the reader is referred to the work of Eddowes,[23] where an analytical solution for the steady-state response of an enzyme-modified pH-sensitive ion-selective device in the presence of pH buffer is derived.

10.3.4 Transient Responses of the ISFET

So far, we have described the pH response of ISFET devices in presence of a fixed electrolyte concentration. We now consider a different situation where a transient variation in such a concentration takes place. To fix ideas, let us assume that an ISFET is immersed in a KCl solution, which increases at $t = t_0$ from concentration C_1 to concentration C_2 during the time interval $\Delta t = t_1 - t_0$. The whole process includes two distinct situations, namely: an *equilibrium* situation for $t < t_0$ and for $t > t_1$, and a *nonequilibrium* situation in the interval Δt. In both situations, the specific value of the ion concentration will affect the surface electric potential φ_{eo}. Under equilibrium conditions, the surface potential can be calculated by solving the corresponding Poisson-Boltzmann equation, developed in Sec. 7.2.1. It can be shown[24] that *very large* changes in the electrolyte concentration, result into *very small* changes in the potential. This means that the static pH response of an ISFET having the appropriate insulator (e.g., Si_3N_4, Al_2O_3, or Ta_2O_5) should be not influenced by the value of the electrolyte concentration.

The transient situation can be quite different from the equilibrium one if the electrolyte concentration is increased in a fast way (i.e., with an "ion step"[24]). In this case, the integral diffuse capacitance $C_d = \sigma_d/\varphi_{eo}$ increases very fast because of the sudden increase in the electrolyte concentration. The charge density σ_d at the insulator surface [see Eq. (10.18)], being unaffected by the ion step, this will result in a decrease in the surface potential φ_{eo}, according to

$$\sigma_d = \varphi_{eo}C_d \tag{10.52}$$

We can then expect a decrease in the surface concentration of protons, H_s^+, as a consequence of the decrease in the potential. However, the ISFET insulator acts as a very good buffer for H_s^+ and it will keep the H_s^+ concentration constant by dissociating more A-OH groups, causing a change in σ_d, so that a new equilibrium is reached when σ_d/C_d reaches the same value as before the ion step. The speed of this process will depend on the diffusion of the H^+ ions and also on the buffer capacity of the system. Data reported in literature indicate that the transient response of a Ta_2O_5 ISFET to a 10- to 50-mM KCl step develops for about 2 s, with a peak value of about 35 mV.[24] This analysis can then be extended to study the ISFET transient response in the presence of biological material. For instance, the presence of layers of charged proteins entrapped in proximity to the ISFET insulator should modify the transient response of an ISFET to an ion step. This statement is based on the fact that the fixed protein charge should introduce a Donnan equilibrium potential (see Sec. 7.3.4) into the electrolyte-ISFET system. As a consequence, the ion-step method could be used to measure and characterize specific proteins (e.g., antibodies).

Up to now we considered ion steps as an input introduced by the experimenter. On the other hand, ion steps can be introduced spontaneously by living biological systems. As will be discussed in detail in Chap. 11, the electrophysiological activity of a neuron is precisely based on transient charge movements at the surface of its membrane. This means that an ISFET brought in proximity to an active neuron should be able to measure its activity, thus forming a *neuroelectronic junction.* This fact, first indicated in a pioneering paper by Bergveld[14] have been confirmed both experimentally[25] and via computer simulation.[26]

In view of its bioelectronic relevance, this topic will be further considered in Secs. 11.6 and 12.4.1.

10.3.5 Modes of Operation of the ISFET

From the analysis of the FET-based biosensor structures, it follows that the main characteristic of the device response is a change in the drain current due to the activity at the insulator gate region. Under the condition of strong inversion (see Sec. 9.1), a change in the activity of the protons in solution gives rise to a change in the concentration of mobile carriers in the channel and thus, for a given constant drain voltage V_{DS}, a change in the drain current I_{DS}.

We can consider two modes of operation:

- V_{GS} and V_{DS} constant; I_{DS} measured.
- I_{DS} and V_{DS} constant; V_{GS} measured.

Operation with Constant $\mathbf{V_{GS}}$. Under this mode of operation, the externally applied voltages (V_{DS} and V_{GS}) are kept constant and I_{DS} is measured by an operational amplifier in the current-to-voltage converter mode (Fig. 10.10*a*), with the gain control of the output signal given with the feedback resistor R_F, such that

$$V_{\text{out}} = -R_F I_{DS} \tag{10.53}$$

In practice, however, V_{out} does not directly reflect I_{DS}, but takes into account also the series resistance of the source and drain regions, causing deviations from linear behavior. The device must therefore be arranged in order to account for these deviations.

Operation with Constant $\mathbf{I_{DS}}$. The circuit of Fig. 10.10a can be modified (Fig. 10.10*b*), so that the output voltage V_{out} provides the control of V_{GS} to keep I_{DS} constant. The volt-

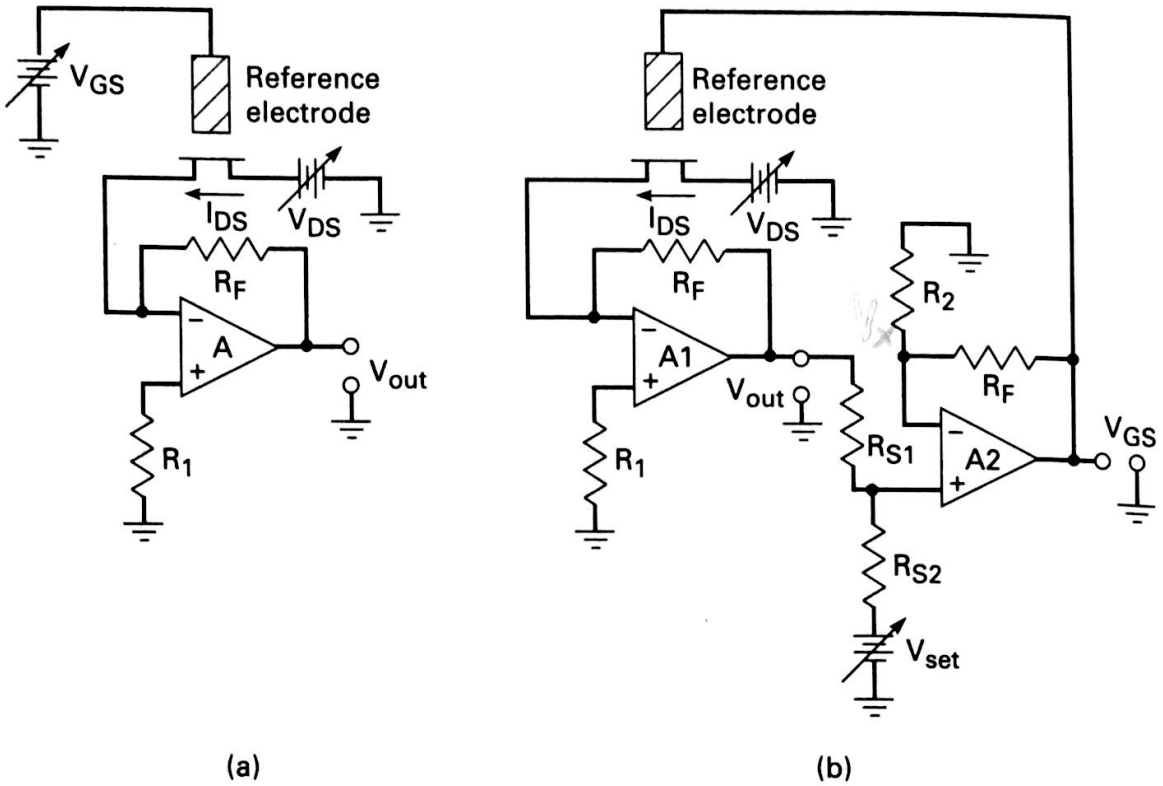

FIGURE 10.10 Modes of operation for MOSFET-based biosensors. Basic circuit for operation with (*a*) constant V_{GS}; (*b*) constant I_{DS}.

age V_{out} is fed through a voltage divider into a differential amplifier, where the inverting input is kept at 0 V, such that 0 V at the noninverting input must be achieved by

$$V_{out} + V_{set} = 0 \tag{10.54}$$

and since

$$I_{DS} = -\frac{V_{out}}{R_F} \tag{10.55}$$

then

$$I_{DS} = \frac{V_{set}}{R_F} \tag{10.56}$$

and the required I_{DS} can be set by acting on V_{set}, so that the output from the differential amplifier will control V_{GS} to obtain the desired constant drain current.

This mode of operation has the advantage that changes in the interface potential can be measured directly. Any change in the value of the term (kT/q) ln $[H^+]$ contributing to I_{DS} will be balanced by an adjustment of V_{GS}.

10.4 CELL-BASED BIOSENSORS AND SENSORS OF CELL METABOLISM

In the mid-1970s it was found that not only enzymes but also whole living microbial cells with their enzyme activity could be used to make biosensors. The first cell-based biosen-

sor was the microbial electrode with the cells of *Acetobacter xylinum* immobilized in a cellulose membrane on the surface of an oxygen electrode. It was used to measure ethanol concentrations on the basis of the measurement of oxygen consumption during ethanol assimilation in bacterial cells. In the following years other microbial biosensors were developed, using the high activity of specific enzymes within the cells of various bacterial and yeast strains. Later on, other types of living cells, and even tissue slices from organs of animals and higher plants, were also used to make biosensors.

The reader can find a wide description of these devices in Ref. 27. In this section we introduce only the main properties of the cell-based biosensors, pointing out their differences with respect to the enzyme-based biosensors.

Cell-based biosensors are then analytical devices, where suitable cells (used as a receptor) are coupled with a transducer. The high enzyme activity within the cells is usually used; the enzyme catalyzes the conversion of a given substrate, and the transducer follows the resulting product with a change of its signal, which is registered by ad hoc electronic equipment. The function of most cell-based biosensors is thus analogous to that of biosensors with immobilized isolated enzymes. However, the use of whole cells has some advantages in comparison with enzyme biosensors. They can be summarized as follows[27]:

1. Cultivation of microbial cells, or preparation of tissue slices in the laboratory, is easy and cheap compared to the preparation of a pure enzyme.
2. Isolation, purification, and immobilization of enzymes are often very difficult; these problems can be eliminated by the use of the whole cells.
3. Some enzymes can lose their activity during isolation or immobilization process; this problem is also eliminated by the use of the whole cells.
4. Enzymes in the cell's natural environment are usually extremely stable.
5. Multistep enzyme reactions in intact cells can be used, making it possible to avoid the preparation of complicated artificial multienzyme systems.
6. Coenzymes and activators are often present in the cells, and thus it is not necessary to add them into the system; the cell itself usually regenerates them.

The use of whole cells for preparation of biosensors has, however, also some disadvantages that can be summarized as follows[27]:

1. The enzyme-catalyzed reaction can take place more slowly because the substrate must cross the cell membrane in order to reach the enzyme, as does the product in order to leave the cell and reach the transducer. Then substrates, especially macromolecular compounds, that are not able to cross the membrane cannot be used.
2. Other metabolic pathways in the cells can be the source of the side products that are also measured by a transducer; this leads to the decrease of the biosensor selectivity.

Cell-based biosensors are usually classified according to:

- *Type of cells* used: the most common are bacterial or yeast cells (*microbial biosensors*); multicellular organisms such as lichens, tissues of higher plants, and animals are also used (*tissue biosensors*).
- *Relation of the cells* to the transducer: *membrane biosensors,* which have the biocatalyzer in the form of a membrane containing the cell suspension or in the form of a tissue slice that is kept on the transducer surface, and *reactor biosensors,* which usually use a suspension of bacterial cells or of plant tissues in a vessel reactor.
- *Transducer type:* the transducer is usually represented by an ion-selective electrode that changes its potential according to the increase of the ion concentration due to the

enzyme, which catalyzes the conversion of the measured substrate. Another possibility is an amperometric detection of substances that can be oxidized on an anode or reduced on a cathode. A further possibility of electrochemical detection is represented by the use of the ISFET.

A different way of considering cell-based biosensors involves detecting changes in the physiological state of cultured living cells by monitoring the rate at which they excrete acidic products of metabolism. Metabolic rate can be defined in various ways: for example, one can monitor the rate of uptake of reactants such as glucose or O_2, or the rate of production of products such as heat, or the acidic products of metabolism, lactic acid and CO_2. An alternative technique, proposed in Ref. 28, consists in measuring extracellular acidification rates: this choice has been made also because of the availability of MOSFET-based biosensors, a technology that is particularly well suited for such measurements. Thus, one measures the rate of pH change of the extracellular medium, which depends on the rate of proton production by cells (e.g., on the order of $10^8 H^+ s^{-1}$ per cell in mammalian cells) and on the buffer capacity of the medium.

Since cells excrete protons into buffered solutions and potentiometric methods detect pH rather than $[H^+]$ directly, it is important to establish the relationship between the number of protons n excreted into a volume V and the resulting pH change. If we assume that the medium is buffered by a weak acid HA present in total concentration $A_{tot} = [HA] + [A^-]$, with dissociation constant K, the buffer capacity β is given by (see Sec. 4.2.2)

$$\beta \equiv -\frac{d(n/V)}{d\text{pH}} = \ln(10)\, A_{tot} \frac{10^{(pK-\text{pH})}}{(1 + 10^{(pK-\text{pH})})^2} \tag{10.57}$$

10.5 LIGHT-ADDRESSABLE POTENTIOMETRIC SENSOR (LAPS)

We have seen in the previous sections that biochemical reactions can be measured potentiometrically through changes in pH. An electronic device, based on the measure of an alternate photocurrent through an electrolyte-insulator-semiconductor (EIS) interface, has been proposed[29] to provide a highly sensitive means to measure such potential changes: such a structure is called *light-addressable potentiometric sensor* (LAPS).

In the following, we provide only the principles of operation mechanisms of LAPS, rather than a quantitative analysis of the device behavior.

10.5.1 LAPS Operation Mechanisms

The LAPS consists mainly of an insulator (usually Si_3N_4) which separates a silicon substrate from an electrolyte (assumed to have a resistance R_e), which is in contact with a controlling electrode to which a bias potential V_{bias} is applied with respect to the substrate of the semiconductor, as shown in Fig. 10.11*a*.

One or more infrared light-emitting diodes (LEDs) are placed just below the semiconductor, and when they are modulated by an alternating signal, a current of photogenerated hole-electron pairs is induced in the circuit. Discrete chemistries can be located on different regions of the insulating surface, producing variations in the local surface potential that can be determined by selective illumination with one or another of the light-emitting diodes (*light addressability*). The photocurrent I_m is the parameter being measured (usually as an rms value).

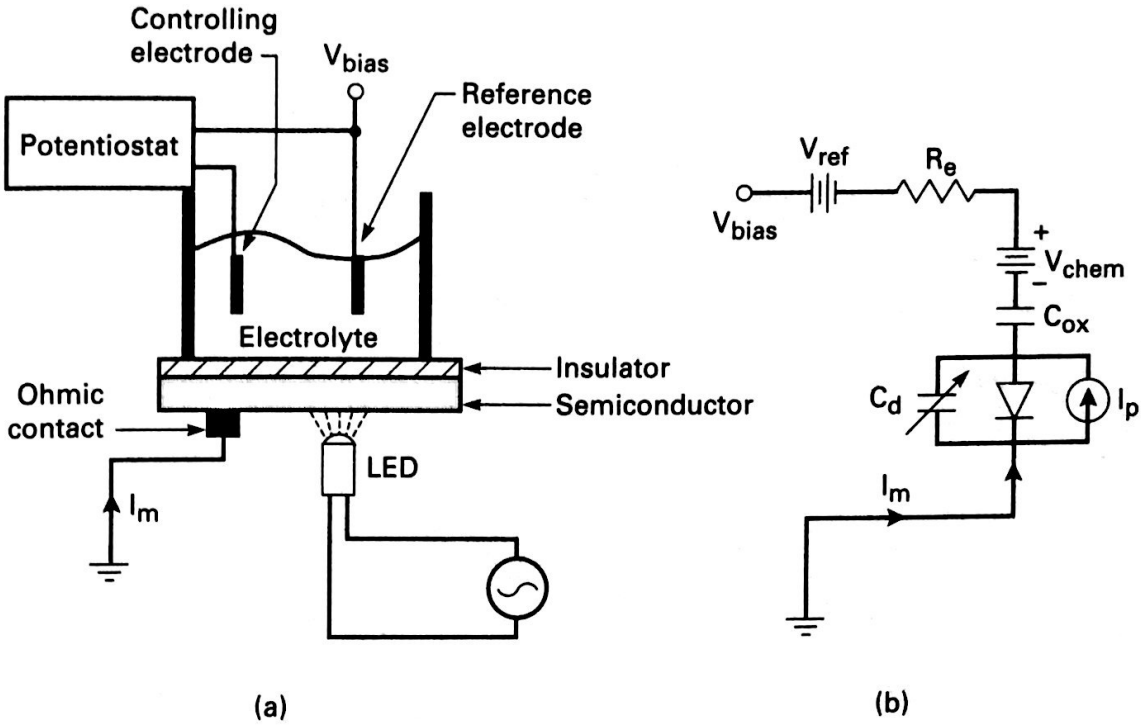

FIGURE 10.11 LAPS. (*a*) Schematic structure and (*b*) simplified equivalent electronic circuit.

In *absence of illumination,* the LAPS behaves like an MOS capacitor (see Chap. 8). For an *n*-type semiconductor, a positive bias potential V_{bias} applied to the structure of Fig. 10.11*a* will drive the semiconductor into accumulation (see Sec. 8.2). Majority carriers (electrons) will distribute uniformly in the semiconductor except at the semiconductor-insulator (SI) interface, where negative charges accumulate to balance the charge at the electrolyte-insulator (EI) interface. In accumulation, the structure is then analogous to a capacitor C_{ox} made of two parallel metal plates separated by the insulator, whose value is given by Eq. (8.2).

If now a negative bias potential V_{bias} is applied to the structure, electrons are driven away from the SI interface, causing a region depleted of majority carriers to appear. We say that the semiconductor is driven into depletion (see Sec. 8.3). The depletion region can be modeled as an insulator with a width that is a function of the bias potential, and it can be represented by a depletion region capacitance C_d. As V_{bias} becomes more negative, the depletion region width [see Eq. (8.17)] increases (and C_d decreases) until it reaches its maximum value.

In *presence of illumination* of the semiconductor of the LAPS with infrared light, there is a generation of hole-electron pairs in the semiconductor, where they can diffuse, recombine, or be separated in an electric field.

When the semiconductor is driven into depletion, hole-electron pairs that have diffused into the depletion region, or that are produced in this region, are separated in the electric field on a time scale short compared to that for recombination.

When the semiconductor is illuminated with a *constant-intensity light* source, charge separation of photogenerated hole-electron pairs in the depletion region gives rise to a transient current which acts to collapse the depletion region and charge the insulator. This current decays as the depletion region width reaches a new steady-state value. Turning off the illumination produces a transient current of opposite polarity as the insulator discharges and the depletion region returns to its original width.

If the *intensity* of the light source is *modulated* with a period short with respect to the

decay time constants of the transient currents, an alternating current is produced because there is never enough flow of charges in either direction to significantly modulate the depletion region width.[30]

Figure 10.11*b* shows a simplified equivalent electronic circuit for the LAPS under photoexcitation produced by an intensity-modulated LED. Modulating the light intensity at a frequency ν results in alternating charging currents through the insulator and depletion region capacitances at the same frequency. The amplitude $|I_m|$ of the insulator charging current through the external circuit is the quantity to be measured. Under *strong depletion,* the measured alternating photocurrent $|I_m|$ is a function of the rate at which hole-electron pairs form in, or diffuse into, the depletion region and of the capacitances of the illuminated area, as given by[30]

$$|I_m| = \frac{C_{ox}}{C_{ox} + C_d}|I_p| \tag{10.58}$$

where $|I_p|$ is the alternating component of I_p, which represents the photogeneration of hole-electron pairs.

When the semiconductor is biased into *accumulation,* although charge separation takes place, there is a small current in the external circuit due to the large value of C_d and the low resistance to charge recombination across C_d (represented by the diode in Fig. 10.11*b*).

Figure 10.12 shows typical sigmoidal shape curves of $|I_m|$ versus V_{bias}. At the most positive bias potential, the semiconductor is in accumulation and no photocurrent is measured. As the semiconductor is driven into depletion, $|I_m|$ increases as C_d decreases. When the maximum depletion width is reached, $|I_m|$ reaches a maximum value.

The LAPS can be used to measure chemically sensitive surface potentials (V_{chem} in Fig. 10.11*b*) on the insulator surface. For example, the potential of a surface with proton binding capacity, will increase on addition of H^+; therefore, on dropping the pH, the bias potential must be decreased to keep the same electrical field in the semiconductor and hence the same photocurrent I_m. As a consequence, there is a shift of the $|I_m|$ versus V_{bias} curves along the V_{bias} axis due to changing the pH, as shown in Fig. 10.12.

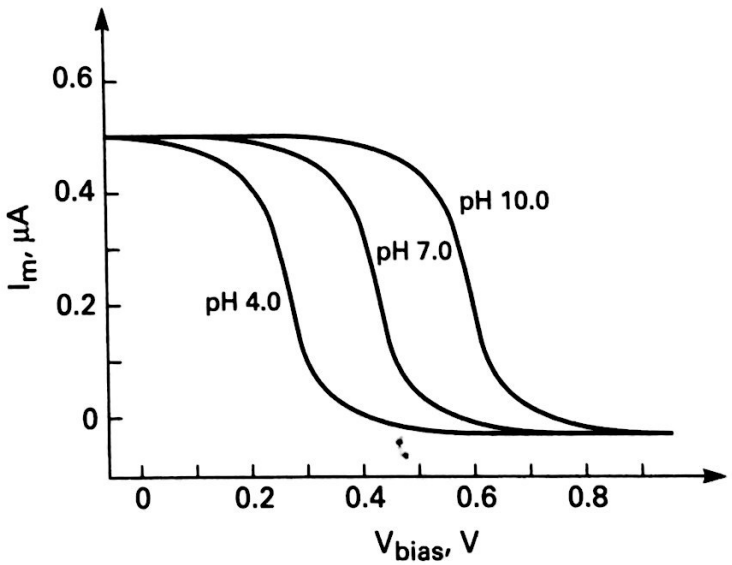

FIGURE 10.12 Alternating photocurrent I_m as a function of bias potential V_{bias} for different values of pH. The curves shown are for *n*-type silicon; for *p*-type silicon the shape of the curve is reversed, left to right.

10.6 CONTRIBUTIONS OF MICROFABRICATION TECHNOLOGIES TO THE FIELD OF BIOSENSORS

Two issues will be shortly addressed in this section, both related to silicon microfabrication techniques, namely:

1. The use of photolithographic techniques and surface chemistry to transform a solid surface (e.g., silicon or gold) into a pattern of micrometer-sized regions with different sensing properties.
2. The exploitation of the mechanical properties of silicon microcantilevers to obtain sensors able to transduce energy changes into bending.

10.6.1 Surface Patterning

One of the key issues in the development of biosensors and arrays of biosensors is the *patterning of surfaces* with complex organic functional groups, including distinct attachment points for proteins, peptides, and carbohydrates.

Surface patterning can be achieved by making use of *photolithography,* a technique routinely used in microelectronics for the fabrication of integrated circuits. In the photolithographic process, a surface is exposed to UV light through a mask in such a way that predetermined, micrometer-sized regions of the surface are alternately exposed to or protected from UV light. In this way, molecules anchored to specific regions of the surface are appropriately modified by the UV light, while other molecules belonging to other regions are not, according to the pattern of the mask. A sequence of masks can be used to generate, as a final result, an array of micrometer-sized regions, each of them with a specific chemistry on it. This methodology is known as *combinatorial chemistry,* and it combines solid-phase synthesis, photolabile protecting groups, and photolithography. Some features of this methodology are illustrated in Fig. 10.13.[31]

Of special interest for the field of biosensors is the use of *self-assembled monolayers* (SAMS) to functionalize the patterned regions. The system of self-assembled monolayers of *alkanethiols*[32] on gold is probably the best chemical system to be utilized in the development of arrays of biosensors. The structure of these monolayers is as follows: the chemisorption of the *thiolsulfur* atoms onto the gold substrate drives the self-assembly of the alkanethiols. The density of the sulfur head groups brings the alkyl backbones of these molecules into close contact, causing the chains to order into a densely packed monolayer with very few defects. Monolayers of alkanethiols on gold are stable for a period of several months in air, or in contact with water or ethanol. They are sufficiently stable for many applications dealing with biosurfaces and have been used for studies of protein adsorption and cell adhesion in aqueous media. Both aspects are of great relevance for the field of biosensors. The adsorption of specific proteins is achieved via the insertion of appropriate functional groups on the portion of the thiols exposed to the solution (see Fig. 10.14). Such functional groups include alkyl, perfluoroalkyl, amide, ester, alcohol, nitrile, carboxylic acid, phosphoric acid, boric acid, amine, and heterocycle groups.

10.6.2 Silicon Microcantilevers

The scanning force microscope (SFM), also known as the atomic force microscope (AFM), was first introduced in 1986.[33] Very briefly, it consists of a Si_3N_4 microcantilever, typically

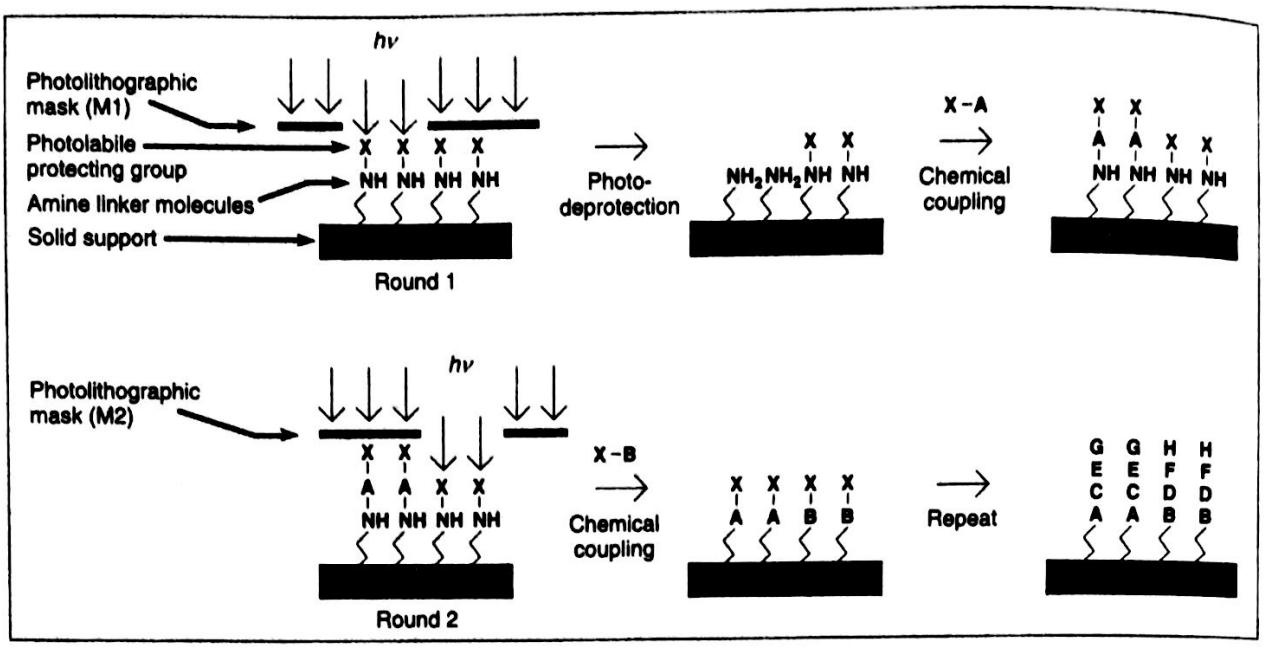

(a)

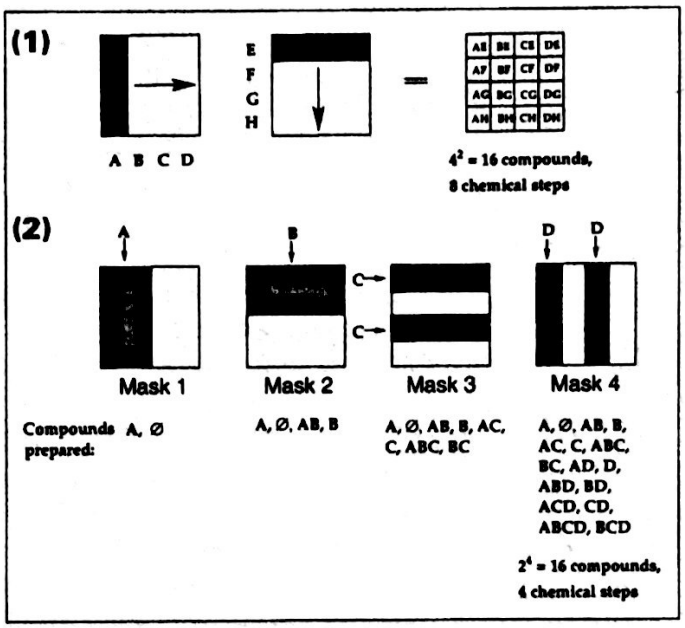

(b)

FIGURE 10.13 (*a*) Light-directed parallel chemical synthesis. A surface is derivatized with amine linkers that are blocked by a photochemically cleavable protecting group. The surface is selectively irradiated with light to liberate free amines, which can be coupled to photochemically protected building blocks. The process is repeated with different regions of the synthesis surface being exposed to light, until a desired array of compounds is prepared. The patterns of photolysis and the order of addition of building blocks define the products and their locations. (*b*) Synthesis strategies: (1) Orthogonal-stripe method. A layer of monomers is formed by photolyzing stripes for each building block. Dimers are formed by photolyzing stripes orthogonal to the first set, preparing n^2 compounds in $2n$ chemical steps. (2) Binary synthesis. Half of the synthesis surface is photolyzed during each coupling step, with subsequent photochemical steps overlapping one-half of the previous synthesis space. With this strategy, 2^n compounds are made in n chemical steps. (*From J. W. Jacobs and S. P. A. Fodor.*[31])

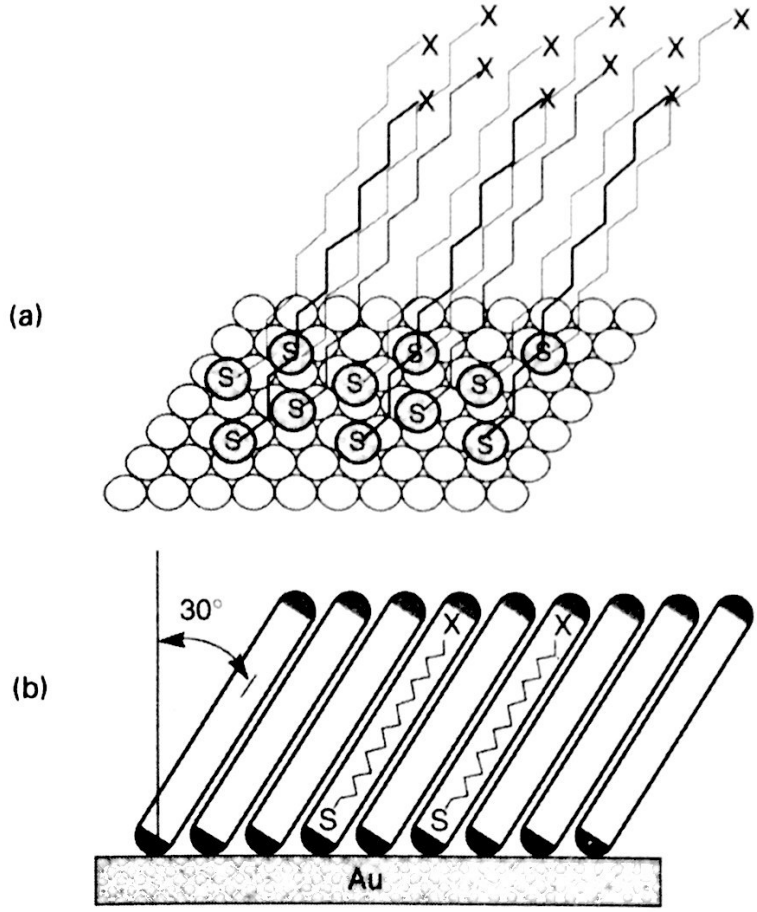

FIGURE 10.14 Representation of a self-assembled monolayer (SAM) of alkanethiolates on the surface of gold. (*a*) The sulfur atoms (S) of the alkanethiolates coordinate to the hollow three-fold sites of the gold (1,1,1) surface; the gold atoms (open circles) are arranged in a hexagonal relationship. The alkyl chains are close packed and tilted approximately 30° from the normal to the surface. (*b*) The properties of the SAM are controlled by changing the length of the alkyl chain and the terminal functional group X of the precursor alkanethiol. (*From M. Mrksich and G. M. Whitesides.*[32])

100 to 300 μm long, 10 to 40 μm wide, and with a thickness in the order of 0.5 to 1 μm. Microelectronic techniques such as etching are utilized in order to form a silicon nitride *tip* at the end of the microcantilever, with radius of the tip (approximated as a half-sphere) in the order of 50 nm. The cantilever-tip system is then driven (with a precision better than 0.1 nm) by piezoelectric motors to scan a surface, and the tip-surface interaction forces, typically in the order of a few nanonewtons, are optically detected by exploiting the fact that the force-induced bending of the microcantilever is amplified by deflecting a light beam generated by a laser impinging on the back of the cantilever. For the purposes of this section, from now on we will focus on the silicon microcantilever *bending* as a consequence of its interactions with the surroundings, without discussing any more the operating principles and the remarkable achievements of SFM, which are described, for example, in Ref. 34. A microcantilever can be viewed as a highly sensitive sensor which can be used to detect the presence of very small amounts of materials both in the gaseous and liquid phase. Two interesting examples of application of this concept are the following.

Detection of Temperature Changes. Aluminum (Al) and silicon nitride (Si_3N_4) present different thermal expansion coefficients. Because of this difference, an Si_3N_4 microcantilever with an Al-coated surface will bend when heat is produced in its proximity. For

uniform heating, the bending z is proportional to the absorbed heating power and is expressed by

$$z = \frac{5}{4}(\alpha_1 - \alpha_2)\frac{t_1 + t_2}{Kt_2^2}\frac{l^3}{W(\lambda_1 t_1 + \lambda_2 t_2)}P \tag{10.59}$$

where[35] K = device parameter
α = expansion coefficient
t and λ = thickness and thermal conductivities of the two layers (i.e., Al and Si_3N_4), respectively
l and W = length and width of the microcantilever
P = total power impinging on the bi-material cantilever

Such a cantilever can then be used as an *ultrasensitive calorimeter* for investigating surface catalytic reactions. Further applications include the detection of the heat involved in phase transitions of picoliter volumes of solid materials, with a resolution in the order of femtojoules under ambient conditions.[35]

Detection of Surface Stress. Measuring the bending of a plate to determine the surface stress σ in thin films is a common technique. Given a microcantilever with two different opposite faces (e.g., one face Si_3N_4, the other one coated with gold), experiencing two different surface stress variations $\Delta\sigma_1$ and $\Delta\sigma_2$, the radius of curvature R of the cantilever is related to the differences in surface stress by

$$\frac{1}{R} = 6\frac{1-\nu}{Et^2}(\Delta\sigma_1 - \Delta\sigma_2) \tag{10.60}$$

where E = Young elasticity modulus of the basic cantilever material (i.e., Si_3N_4)
ν = Poisson ratio
t = thickness of the cantilever

Equation (10.60) implies that a microcantilever with appropriately prepared opposite faces will *bend* as a result of changes of stress on the two surfaces. Suppose an Si_3N_4 cantilever is coated with gold on the upper surface and then is immersed in a liquid solution with a given pH. As already discussed in Chaps. 7 and 10, an Si_3N_4 surface presents a charge density which is a function of the H^+ ions present in solution. We can further assume negligible pH-dependent charges on the Au surface. As a whole, we can then predict changes in cantilever deflection and surface stress when varying the pH in an aqueous solution. The cantilever thus can become an unconventional, micrometer-sized pH sensor.[36] Moreover, the gold surface can be coated with a self-assembled monolayer of alkanethiol molecules appropriately functionalized with functional groups (see previous section). The interaction with specific molecules present in a liquid solution can then be revealed by a differential stress-induced cantilever bending. As a subsequent step, by evaporating gold also on the free Si_3N_4 surface, monolayers of thiols with different biosensing properties can be assembled on the two surfaces of the cantilever, thus increasing the biological selectivity of the cantilever-based biosensor.[36–38] Arrays of microcantilevers with different coating and thus different sensing properties could result into a micrometer-sized integrated multiple-sensor system.

PROBLEMS

10.1 Consider a Ta_2O_5 ISFET exposed to a 1:1 electrolyte. Assuming $pK_a = 4$, $pK_b = -2$, and a number of surface sites $N_s = 10 \times 10^{14}/cm^2$, find, at $T = 300$ K,